

# DIELECTRIC AND OTHER NON-PLASMA ACCELERATOR BASED COMPACT LIGHT SOURCES\*

R. J. England<sup>†</sup>, Z. Huang

SLAC National Accelerator Laboratory, Menlo Park, CA 94025, USA

## Abstract

We review recent experimental progress in developing nanofabricated dielectric laser-driven accelerators and discuss the possibility of utilizing the unique sub-femtosecond electron pulse format these accelerators would provide to create ultra-compact EUV and X-ray radiation sources.

## INTRODUCTION

Particle acceleration in dielectric structures driven by ultrafast infrared lasers, a technique we refer to as “dielectric laser acceleration” (DLA), is a new and rapidly progressing area of advanced accelerator research that sets the stage for future generations of high-gradient accelerators of reduced cost and unprecedented compactness. In recent years, there have been several critical experiments: the first demonstration of high-field (300 MV/m) speed-of-light electron acceleration in a fused silica structure [1], acceleration at sub-relativistic energies with an open grating [2], demonstration of a compatible optical-scale beam position monitor [3], high-gradient sub-relativistic acceleration at 220 MV/m [4] and at 370 MV/m [5] in silicon microstructures, and high-gradient (700 MV/m) acceleration of relativistic electrons using femtosecond laser pulses [6]. This approach has been colloquially referred to in the press as an “accelerator on a chip.” The high-gradient and wafer size of these accelerators make them very attractive for a future generation of high brilliance extreme ultraviolet (EUV) and X-ray sources. The DLA approach has the distinct features to produce attosecond electron bunches and can operate at 10s of MHz repetition rate. However, there are many accelerator science questions and technical challenges to address since the beam parameters for an accelerator based on this concept would be drastically different from both conventional accelerators and other advanced schemes.

The most powerful XUV and x-ray sources today are enabled by relativistic electron beams driven by state-of-the-art microwave linear accelerator facilities such as the Linac Coherent Light Source (LCLS) at SLAC. Recent research into novel dielectric laser accelerators (DLA) has given rise to the potential for new coherent radiative processes with attosecond pulses using dielectric structures with wavelength-scale periodic features excited by lasers at near-infrared wavelengths [1, 7], and with orders of magnitude higher accelerating fields than is possible with conventional microwave technology [6]. This approach has the potential to produce extremely bright electron beams in an ultra-

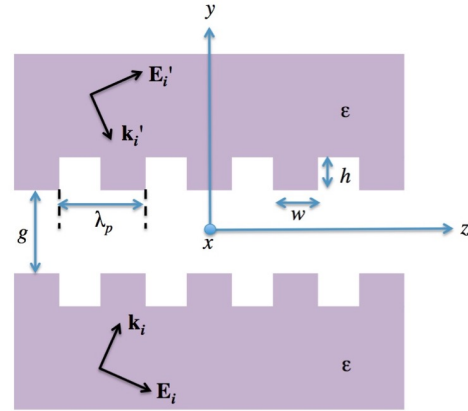


Figure 1: Planar symmetric geometry with periodic variation in  $z$ . Two exciting plane waves are shown incident from top and bottom.

compact footprint that are suitable for driving superradiant EUV light in a similarly optical-scale laser-induced undulator field. Radiation from each undulator/compressor module would add in amplitude but not in pulse length, maintaining the wide bandwidth and attosecond pulse structure. Preliminary calculations presented below suggest that a compact DLA driven by a  $2 \mu\text{m}$  infrared laser may generate a 10-fC, 200-as electron bunch train at 40 MeV particle energy. After passing 100 undulator/compressor modules, EUV radiation could be generated in a train of 660 as pulses separated by 6.6 fs laser period, with a pulse energy of more than 100 nJ. This attosecond pulse train would form an intense EUV frequency comb that would be extremely valuable for precision spectroscopy.

## LASER-DRIVEN DEFLECTION IN PLANAR STRUCTURE

All DLA structures experimentally tested to date have been of the planar symmetric variety (spatially invariant in one coordinate) and with a longitudinal periodicity along the particle beam axis. We here derive a generic form for the transverse forces in such a geometry which provide some helpful insights regarding development of a compatible laser-driven undulator. The wave equation for a linear material with spatially varying dielectric function  $\epsilon(\mathbf{r})$  may be written

$$\nabla^2 \mathbf{E} - \nabla(\nabla \cdot \mathbf{E}) = -(\omega/c)^2 \mathbf{D} \quad (1)$$

where  $\mathbf{D}$  is the electric displacement field, related to the electric field  $\mathbf{E}$  and polarization  $\mathbf{P}$  by  $\mathbf{D} = \mathbf{E} + 4\pi\mathbf{P}$ . We assume a dielectric, non-magnetic material ( $\mu = 1$ ), hence  $\mathbf{H} = \mathbf{B}$ . Solutions to Eq. 1 for given dielectric function

Content from this work may be used under the terms of the CC BY 3.0 licence (© 2018). Any distribution of this work must maintain attribution to the author(s), title of the work, publisher, and DOI.

\* Work supported by U.S. Dept. of Energy, National Science Foundation, and Moore Foundation.

<sup>†</sup> england@slac.stanford.edu

$\epsilon(\mathbf{r})$  immediately yield the magnetic field via Faraday's law,  $\nabla \times \mathbf{E} = i(\omega/c)\mathbf{B}$ . By the Floquet theorem, the solutions to Maxwell's equations subject to periodic boundary conditions along  $z$  with periodicity  $\mathbf{u} = \lambda_p \hat{\mathbf{z}}$  satisfy  $\mathbf{E}(\mathbf{r} + \mathbf{u}) = \mathbf{E}(\mathbf{r})e^{i\psi}$ , where  $\psi$  is the cell-to-cell phase shift. If the fields are excited by an incident plane wave with wavenumber  $\mathbf{k}_i = (\omega/c)\sqrt{\epsilon_i} \hat{\mathbf{n}}$ , then  $\psi$  is given by the projection of the incident plane wave onto the fundamental periodicity. If we define  $\theta$  to be the usual polar angle between  $\hat{\mathbf{n}}$  and  $\hat{\mathbf{z}}$  then this gives rise to the projection of the incident wave in the first Brillouin zone:  $k_0 \equiv |\mathbf{k}_i \cdot \mathbf{u}| = (\omega/c)\sqrt{\epsilon_i} \cos \theta$ , and a corresponding set of Floquet space harmonics with wave numbers  $k_n = k_0 + nk_p$  where  $k_p \equiv 2\pi/\lambda_p$ . The phase velocity of the  $n$ 'th space harmonic, normalized to speed of light  $c$  is thus  $\beta_n = \omega/(ck_n)$ .

For the considered case, illustrated in Fig. 1 by the example of parallel gratings with rectangular teeth, with a planar-symmetric system invariant in  $x$ , and a vacuum region occupying the space  $|y| < g/2$ , two orthogonal polarizations may be defined relative to the plane of  $y$  and  $z$  wherein there is variation of the fields. We call these S and P polarization, which respectively give rise to transverse electric (TE) and transverse magnetic (TM) modes, relative to excited surface waves propagating in  $z$  within the vacuum gap. For a single laser excitation ( $\mathbf{E}_i$  in Fig. 1), the solution to Eq. 1 in the vacuum region yields the following non-vanishing components for S- polarization (TE):

$$\begin{aligned} E_x &= E_0 \sum_n [a_n e^{\Gamma_n y} + b_n e^{-\Gamma_n y}] e^{ik_n z} \\ B_y &= \frac{c}{\omega} E_0 \sum_n k_n [a_n e^{\Gamma_n y} + b_n e^{-\Gamma_n y}] e^{ik_n z} \\ B_z &= i \frac{c}{\omega} E_0 \sum_n \Gamma_n [a_n e^{\Gamma_n y} - b_n e^{-\Gamma_n y}] e^{ik_n z} \end{aligned} \quad (2)$$

and for P-polarization (TM):

$$\begin{aligned} E_y &= -iE_0 \sum_n \frac{k_n}{\Gamma_n} [a_n e^{\Gamma_n y} - b_n e^{-\Gamma_n y}] e^{ik_n z} \\ E_z &= \frac{c}{\omega} E_0 \sum_n k_n [a_n e^{\Gamma_n y} + b_n e^{-\Gamma_n y}] e^{ik_n z} \\ B_x &= iE_0 \sum_n \frac{\omega}{c} \frac{1}{\Gamma_n} [a_n e^{\Gamma_n y} - b_n e^{-\Gamma_n y}] e^{ik_n z} \end{aligned} \quad (3)$$

where  $\Gamma_n \equiv \sqrt{k_n^2 - (\omega/c)^2}$  is the transverse decay constant of the  $n$ 'th space harmonic. The complex coefficients  $a_n, b_n$  are determined by boundary condition matching at the dielectric interface and therefore depend upon the specific geometry of the periodic structure. Explicit forms have been derived for a square-tooth grating as depicted in Fig. 1 by, e.g. [8,9]. By virtue of the assumed symmetry, if an otherwise identical plane wave  $\mathbf{E}'_i$  propagates from the opposite direction with the same incidence angle, then the resultant mode is of the same form as Eqs. 2 - 3 but with the substitution  $a_n \leftrightarrow b_n$ .

The superposition of the fields excited by both plane waves has the form of Eqs. 2 - 3 but with the replacements

$$[a_n e^{\Gamma_n y} \pm b_n e^{-\Gamma_n y}] \rightarrow 2(a_n + b_n) \begin{cases} \cosh(\Gamma_n y) \\ \sinh(\Gamma_n y) \end{cases} \quad (4)$$

If the two plane-waves are out of phase by  $\pi$  then the roles of cosh and sinh in Eq. 4 are exchanged and  $(a_n + b_n) \rightarrow (a_n - b_n)$ . The desired acceleration mode is the in-phase TM mode with  $n = 1$ , wherein  $E_z \propto \cosh(\Gamma y) e^{ik_p z}$ . The hyperbolic cosine dependence can be seen to approach a transversely uniform field in the limit where  $g \ll \Gamma_n^{-1}$  or the case  $\Gamma_n \rightarrow 0$  which implies that  $k_n = \omega/c$  and hence that the phase velocity of the mode is equal to  $c$ . To instead obtain a uniform deflecting force, we consider modes where the transverse force  $\mathbf{F}_\perp$  has a cosh-like dependence on  $y$ . From the above considerations we see that two solutions satisfy this condition: the double-sided excitation of TM mode with  $\pi$  out-of-phase plane waves and the TE mode with in-phase plane waves. These yield

$$\mathbf{F}_\perp = qE_0 \begin{Bmatrix} (1 - \beta/\beta_n) \\ -i \frac{k_n}{\Gamma_n} (1 - \beta_n \beta) \end{Bmatrix} \begin{Bmatrix} \hat{\mathbf{x}} \\ \hat{\mathbf{y}} \end{Bmatrix} e^{i(k_n z - \omega t)} \quad (5)$$

where the top line corresponds to the TE mode and the bottom line is the TM mode. In both cases  $F_z = 0$ . We have here taken a single mode  $n$  from the summation which is assumed to have a phase velocity  $\beta_n$  that is matched to the electron beam, and have assumed the limit  $\Gamma_n g \ll 1$  or  $\cosh(\Gamma_n y) \approx 1$ . Further the constant  $a_n \pm b_n$  has been absorbed into the field amplitude  $E_0$ . We see from these expressions that the TE mode vanishes for a synchronous particle ( $\beta = \beta_n$ ) while the TM mode instead scales as  $1/\gamma_n^2$ . Pletner solves this speed-of-light synchronicity problem by rotating the particle axis by an angle  $\alpha$ . In the rotated frame of the beam, the resonant velocity of the mode is in the direction of  $\mathbf{k}_n$  which is no longer co-linear with  $z$  but now has the form  $\mathbf{k}_n = k_n(\cos \alpha \hat{\mathbf{z}} - \sin \alpha \hat{\mathbf{x}})$ . Phase synchronicity is therefore accomplished if  $\mathbf{k}_n \cdot \hat{\mathbf{z}} = \omega/\beta c$ . For normal laser incidence ( $\theta = \pi/2$ ) this leads to the synchronicity condition  $\lambda_p = \beta n \lambda \cos \alpha$ . Hence, as compared with the unrotated case, the period  $\lambda_p$  of the grating must be decreased by a factor  $\cos \alpha$  to remain synchronous with a speed of light particle. This is geometrically obvious since in the rotated frame the apparent spacing between grating teeth is increased along  $z$ . Laser-driven dielectric undulators based upon this and similar concepts have been proposed and could attain very short (mm to sub-mm) periods with multi-Tesla field strengths and fabricated using similar photolithographic methods [10–12].

## ATTOSECOND RADIATION GENERATION

Combining the high gradient and high brightness of advanced accelerators with novel undulator designs would enable laboratory-scale demonstrations of key concepts needed for future EUV and X-ray lasers that can transform the landscape of ultrasmall and ultrafast sciences. Attosecond electron current modulation would be automatically created by

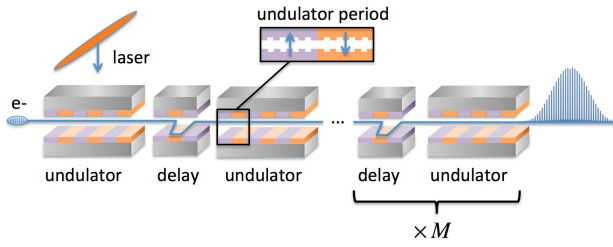


Figure 2: Chain of  $M$  laser-driven undulator and delay modules to mode-lock DLA attosecond pulse train.

the DLA structure and phase-locked to the drive laser. The radiative process could then be modelocked via a chain of such laser-driven undulators and compressors as suggested in [13]. This mode-locked radiation would possess the attosecond pulse structure with a well-defined phase within the train. The undulator and delay chain can be made of dielectric structures as well (see, e.g., Ref. [10, 14]), as illustrated in Fig. 2.

In an operating DLA, the optimal bunch charge would be of order a few fC, so we will ignore the FEL gain in the undulator/delay chain. Following Ref. [13] Sec. 3 we rewrite the equations without  $\rho$  scaling, yielding the radiation field

$$A(\bar{\nu}) = b_0(\bar{\nu})N_u \text{sinc}(\pi\bar{\nu}N_u) \frac{1 - e^{-iM\bar{\nu}\bar{s}}}{1 - e^{-i\bar{\nu}\bar{s}}} e^{-i\bar{\nu}(\bar{s} - \pi N_u)} \quad (6)$$

The corresponding power spectrum is then  $P(\bar{\nu}) \propto |A(\bar{\nu})|^2$ . Here  $\bar{\nu} = (\omega - \omega_0)/\omega_0$  is the undulator fundamental radiation frequency,  $N_u$  is the number of undulator periods per section,  $M$  is the number of sections of undulator/delay modules, and  $\bar{s} = k_0 R_{56}/2 + 2\pi N_u$  is the total slippage per module in units of  $\lambda_0/(2\pi)$ . The quantity  $b_0(\nu)$  is the initial bunching spectrum and is assumed to be constant in the undulator in absence of FEL interaction.

The sinc function shows the typical undulator radiation behavior, with the FWHM spectral width given by  $1/N_u$ . The last factor in Eq. (6) introduces spectral modes. In Fig. 3, we show an example when  $N_u = 5$ ,  $\bar{s} = 2\pi \times 100$ , and  $M = 10$ . About 20 modes are contained in the full spectral bandwidth, and the intensity of the central mode is enhanced by  $M^2 = 100$ .

As discussed in Ref. [13], the mode will not be locked if the electron bunch is randomly distributed, and can be locked if the bunch is energy or density modulated with a modulation wavelength that matches  $\bar{s}/k_0$ . In a DLA, the attosecond bunch train is generated by some sort of an optical buncher so the mode locking happens naturally. The mode-locking means the XUV radiation will possess the attosecond pulse train with a well-defined phase within the train. The peak power of the core part of the train (not head or tail which may be subject to transient effects) can be calculated as follows.

We will work in the 1D limit (assuming a large transverse beam size and can consider 3D later), the transverse electric

field is (see Eq. (3) of Ref. [15])

$$E_x(z, t) = \eta \sum_{j=1}^N \frac{e^{ik_r[z - c(t - t_j)]}}{1 - \beta_{\parallel}} H(z, t - t_j) + \text{c. c.}, \quad (7)$$

where  $\eta \equiv ecZ_0K_{JJ}/8\pi\sigma_x^2\gamma$ ,  $K_{JJ}$  is the undulator parameter with the usual Bessel function correction,  $t_j$  is the electron arrival time at the undulator entrance  $z = 0$ ,  $Z_0 = 377 \Omega$  is the vacuum impedance,  $\beta_{\parallel}$  is the average longitudinal velocity in the undulator,  $\lambda_r = (1 - \beta_{\parallel})\lambda_u$ , and  $H$  is 1 when  $\beta_{\parallel}c(t - t_j) < z < c(t - t_j)$  and 0 otherwise to take care of the slippage. Although this expression is derived in 1D, the electric field transverse distribution should follow that of the electron beam as

$$E_x(z, t, r) = \eta \sum_{j=1}^N \frac{e^{ik_r[z - c(t - t_j)]}}{1 - \beta_{\parallel}} H(z, t - t_j) \times \exp\left(-\frac{r^2}{2\sigma_x^2}\right) + \text{c. c.} \quad (8)$$

In the DLA example we consider here, we assume the DLA bunches the electron to attosecond durations. This is supported by recent VORPAL simulations that show 10 as bunches formed in a 1-mm DLA structure. As far as XUV radiation (tens of nm wavelength) is concerned, the electron bunch radiates coherently right away in the undulator as a macro point charge. This can be seen from the above equation that the sum of phases yields  $N$ , the number of electrons in the attosecond bunch. We have

$$E_x(z, t, r) = \eta \frac{N}{1 - \beta_{\parallel}} e^{ik_r(z - ct)} \exp\left(-\frac{r^2}{2\sigma_x^2}\right) + \text{c. c.} \quad (9)$$

Note that the electric field amplitude is independent of  $N_u$  (undulator period), only the length of the wavepacket is determined by  $N_u\lambda_u$ . This agrees with the intuitive picture. The radiated power per module is given by

$$P_0 = \frac{1}{2Z_0} \int |E_x(z, t, r)|^2 d\mathbf{r} = \frac{Z_0 K_{JJ}^2 Q^2 c^2 \gamma^2}{8\pi\sigma_x^2 (1 + K^2/2)^2}, \quad (10)$$

where  $Q = Ne$  is the total charge in the bunch. After  $M$  modules, the radiated power becomes

$$P = M^2 P_0. \quad (11)$$

For example, consider a compact DLA driven by a 1  $\mu\text{m}$  infrared laser. We assume the charge per bunch is 10 fC, and the fwhm bunch length is 20 as (6 nm) and is shorter than the radiation wavelength (10 nm). Suppose the electrons are accelerated to 50 MeV, and focused to  $\sigma_x = 0.2 \mu\text{m}$  and then passed through a Byer-Plettner type of dielectric undulator with  $\lambda_u = 200 \mu\text{m}$ , and  $K = 0.15$  is the deflecting parameter. The undulator fundamental wavelength is  $\lambda_0 = 10 \text{ nm}$ . Since the electron bunch length is comparable to the radiation wavelength, coherent radiation will be emitted at  $\lambda_0$  from the beginning. After  $N_u = 5$  undulator period, the radiation wavepacket is 50 nm or 166 as. If we simply make the undulator longer, it will only elongate the wavepacket

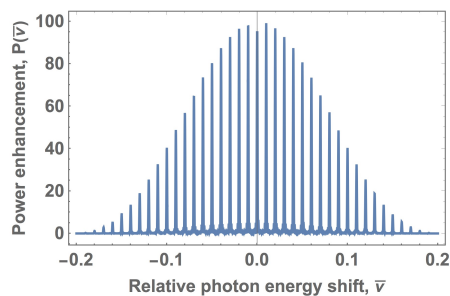


Figure 3: Mode-locked coherent undulator radiation spectrum (see text for details).

and eventually merge the attosecond pulse train. Mode-locking with undulator/chicane module will maintain the wide bandwidth nature and attosecond pulse train. Let us take undulator/chicane module  $R_{56}/2 + N_u \lambda_0 = 1 \mu\text{m}$  to match the drive laser wavelength and hence the periodicity of the bunch train, then the radiation from adjacent modules will add in amplitude but not in pulse duration. After  $M = 10$  such modules, the radiation will maintain 166 as with the peak power given by Eqs. (10) and (11). In this example,  $P = 80 \text{ MW}$ , and the single pulse energy is 13 nJ. If the optical laser pulse length is 1 ps, there can be approximately 300 such pulses in each optical pulse (with some transient effects in head/tail of the optical pulse).

Eventually the beam quality (energy spread) limits how many modules can be used in this scheme. Each chicane/undulator module will have  $R_{56} \sim 2 \mu\text{m}$ , so energy spread requirement is

$$\sigma_\delta M R_{56} < 6 \text{ nm} \quad \text{or} \quad \sigma_\delta < 3 \times 10^{-4}. \quad (12)$$

There should be focusing after each module in order to keep the constant beam size in the undulators. Since the undulator radiation is transversely coherent, the emittance of the bunch should be

$$\epsilon_{x,y} \leq \frac{\lambda_0}{4\pi} \sim 1 \text{ nm}. \quad (13)$$

This corresponds to the normalized emittance  $\gamma \epsilon_{x,y} = 0.1 \mu\text{m}$ .

## APPLICATIONS

The DLA approach can produce orders of magnitude higher accelerating fields than is possible with conventional microwave technology. The extreme accelerating environment has the potential to produce extremely bright electron beams that are suitable for driving superradiant EUV light in a similarly optical-scale laser-induced undulator field. Furthermore, because of the few-femtosecond optical cycle of near infrared (NIR) mode-locked lasers, laser-driven X-ray free electron lasers could allow attosecond x-ray laser pulses to probe matter on even shorter time-scales than possible today. Combining the high gradient and high brightness of advanced accelerators with novel undulator designs could enable laboratory-scale demonstrations of key concepts needed

for future XUV and X-ray lasers that can transform the landscape of ultrasmall and ultrafast sciences. To realize these laboratory-scale, lower-cost, higher performance radiation sources, critical components of laser-driven free electron lasers need to be developed and demonstrated.

Coherent attosecond radiation could potentially be produced using the same operating principles that produce particle acceleration via the “accelerator on a chip” mechanism. These structures operate optimally with optical-scale pulse formats, making high repetition rate (10s of MHz) attosecond-scale pulses a natural combination. The beam is by necessity very close to the exposed micro-structures and there are fundamental questions regarding the impact of the beam impedance upon itself and the remnant fields back on the device itself. This regime has never been studied before and questions arise as to how well the beam will behave in such structures and how well it will ultimately perform. The theoretical and numerical tools to model these processes need to be developed in order to guide experimental studies of attosecond electron and photon generation.

The FEL process has been studied extensively over a broad range of parameters and is quite well understood; however, this is not true in this new regime of ultrashort, attosecond bunches generating X-rays at relatively low electron beam energies. This presents some interesting new opportunities. As the electron energy becomes lower, the impact of the X-ray photon’s momentum on the electron’s momentum becomes significant and quantum effects start to come into play in a way not before seen or measured in “classical” FELs [16]. This has consequences with respect to, among other things, the fundamental physics of coherence between particles, the causal relationships between these particles, and the momentum exchange difference that occurs between incoherent emission and coherent emission. The FEL operated in such a regime might help answer some of these fundamental questions.

## CONCLUSION

A DLA-based light source could generate EUV radiation in the 50 eV photon energy range with even lower beam energies (about 40 MeV using a laser driven undulator with a period of 250  $\mu\text{m}$ ). However, at these relatively long wavelengths, radiation will slip out of the very short electron bunch after of order 10 undulator periods, and hence make the device inefficient for generation of high-power, attosecond (as) pulses. In a DLA, attosecond electron current modulation is automatically created by the structure and is phase-locked to the drive laser which can be further stabilized using optical techniques. One possible route to mode-lock the radiative process via a chain of laser-driven undulators and compressors is suggested in Ref. [13]. If successfully mode-locked, the EUV radiation would possess the attosecond pulse structure with a well-defined phase within the train. Radiation from each undulator/compressor module would add in amplitude but not in pulse length, maintaining the wide bandwidth nature and attosecond pulse train.

This attosecond pulse train would form an intense EUV frequency comb (see Fig. 3) that could be extremely valuable for precision spectroscopy.

## ACKNOWLEDGMENT

This work is supported by the U.S. Department of Energy (DE-AC02-76SF00515), U.S. National Science Foundation (ECS-9731293), and the Moore Foundation (GBMF4744). We also thank R. L. Byer, K. P. Wootton, Y-C. Huang, and L. Schachter for helpful comments and discussions.

## REFERENCES

- [1] E. A. Peralta, K. Soong, et al. "Demonstration of electron acceleration in a laser-driven dielectric microstructure," *Nature* 503, 91-94 (2013).
- [2] J. Breuer and P. Hommelhoff, "Laser-based acceleration of nonrelativistic electrons at a dielectric structure," *Phys. Rev. Lett.* 111, 134803 (2013).
- [3] K. Soong, E. Peralta, et al. "Electron beam position monitor for a dielectric microaccelerator," *Optics Letters* 39 (16), 4747-4750 (2014).
- [4] K. J. Leedle, R. F. Pease, R. L. Byer, and J. S. Harris, "Laser acceleration and deflection of 96.3 keV electrons with a silicon dielectric structure," *Optica* 2, 158-161 (2015).
- [5] K. J. Leedle, A. Ceballos, et al. "Dielectric laser acceleration of sub-100 keV electrons with silicon dual-pillar grating structures," *Optics Letters* 40 (18), 4344 (2015).
- [6] K. Wootton, et al. "Demonstration of acceleration of electrons at a dielectric microstructure using femtosecond laser pulses," *Optics Letters* 41 (12), 2672 (2016).
- [7] R. J. England, et al. "Dielectric Laser Accelerators" *Rev. Mod. Phys.* 86, 1337 (2014).
- [8] L. Pilozzi, A. D'Andrea, and R. Del Sole, "Electromagnetic properties of a dielectric grating I. Propagating, evanescent, and guided waves," *Phys. Rev. B*, 54 (15), 10751 (1996).
- [9] A. Hanuka, W. D. Kimura, I. Pogorelski, and L. Schachter, "Quasi-analytic design of a dielectric acceleration structure," *AIP Conference Proceedings* 1812, 060012 (2017).
- [10] T. Plettner and R. L. Byer, "Proposed dielectric-based microstructure laser-driven undulator," *Phys. Rev. ST Accel. Beams* 11, 030704 (2008).
- [11] F. Toufexis, T. Tang, and S. G. Tantawi, "A 200  $\mu\text{m}$ -period laser-driven undulator," *Proceedings of FEL 2014, Basel, Switzerland* MOP047 (2014).
- [12] K. P. Wootton, et al. "Design and optimisation of dielectric laser deflecting structures," *Proceedings of 2015 International Particle Accelerator Conference (IPAC'15)*, WEPJ012 (2015).
- [13] E. Kur *et al.*, "A wide bandwidth free-electron laser with mode locking using current modulation," *New Journal of Physics* 13, 063012 (2011).
- [14] T. Plettner *et al.*, "Photonic-based laser driven electron beam deflection and focusing structures," *Phys. Rev. ST Accel. Beams* 12, 101302 (2009).
- [15] Z. Huang, K.-J. Kim, "Coherent spontaneous emission in high gain free-electron lasers," *Proceedings of 1999 Particle Accelerator Conference (PAC 1999)*, 2495 (1999).
- [16] R. Bonifacio, N. Piovella, G. R. M. Robb, and A. Schiavi, "Quantum regime of free electron lasers starting from noise," *Phys. Rev. ST - Accel. Beams* 9, 090701 (2006).